Statistical analysis of the relationship between Quasi-Biennial Oscillation and Southern Annular Mode

Fernanda Cerqueira VASCONCELLOS[1], Maria Lívia Lins MATTOS-GAVA[2] and Clovis Angeli SANSIGOLO[2]

[1] *Department of Meteorology, Geosciences Institute, Federal University of Rio de Janeiro (UFRJ), Rio de Janeiro, RJ 21941-916, Brazil.*
[2] *National Institute for Space Research (INPE), São José dos Campos-SP, Brazil.*
*Correspondence author; fernandavasconcellos@igeo.ufrj.br

RESUMEN

El Modo Anular del Sur (SAM) es un patrón extratropical que influye en el clima de todo el hemisferio sur. Sin embargo, la variabilidad de este modo es un área de investigación activa. La influencia de los modos de frecuencia más baja en SAM es un camino hacia un mejor conocimiento sobre este patrón. La relación entre la Oscilación Cuasi-Bienal (QBO) y la contraparte de SAM en el Hemisferio Norte (Modo Anular del Norte) se ha abordado en trabajos anteriores. Aún así, pocos estudios se centran en la asociación entre QBO y SAM. El objetivo de este trabajo fue evaluar la posible relación QBO-SAM mediante análisis estadísticos. Esta asociación se investigó comparando los índices QBO y SAM, este último en diferentes niveles de la tropósfera y la estratósfera, para el período 1981-2010. El análisis de ondeletas mostró que los índices SAM para la tropósfera y la estratósfera presentaban variabilidad en muchas escalas, incluida una banda de dos años. La técnica de ondeletas cruzadas ("*cross-wavelets*") entre QBO y SAM identificó que dicha relación tiene una interacción compleja. Hubo una alta potencia común significativa alrededor de la banda de dos años, con rezagos que variaron durante el período analizado, incluido sin rezago. Un análisis adicional sin rezago confirmó estudios previos, lo que indica que la fase SAM negativa (positiva) es más frecuente para QBO del este (oeste). Sin embargo, esto no fue válido para todos los meses. Algunos análisis adicionales sugirieron que la propagación de ondas ascendentes a la estratósfera para cada fase de QBO cambia el chorro estratosférico y, en consecuencia, la fase de SAM.

ABSTRACT

The Southern Annular Mode (SAM) is an extratropical pattern that influences the climate of all Southern Hemisphere. However, the variability of this mode is an active area of research. The influence of lower frequency modes on SAM is a path to better knowledge about this pattern. The relationship between Quasi-Biennial Oscillation (QBO) and SAM's counterpart in the Northern Hemisphere (Northern Annular Mode) has been addressed by previous work. Still, few studies focus on the association between QBO and SAM. The goal of this work was to evaluate the possible QBO-SAM relationship through statistical analyses. This association was investigated by comparing QBO and SAM indices, the latter on different levels of the troposphere and stratosphere, for the 1981-2010 period. The wavelet analysis showed that the SAM indices for troposphere and stratosphere presented variability in many scales, including a two-year band. Cross-wavelets techniques between QBO and SAM ratified that this relation has a complex interaction. There was a significant common high power around the two-year band, with lags varying over the analyzed period, including no lag. Further analysis without lag confirmed previous studies, indicating that the negative (positive) SAM phase is more frequent for easterly (westerly) QBO. However, this was not valid for all months. Some additional analysis suggested that the upward wave propagation to the stratosphere for each QBO phase changes the stratospheric jet and, consequently, the SAM phase.

1. Introduction

The atmosphere is a complex system with interactions at different temporal and spatial scales. Studies of these interactions are necessary since their influences on atmospheric circulation can explain abnormal events in various regions of the globe. Teleconnection patterns, in which local anomalies influence remote areas, are a great example of this mechanism.

The Quasi-Biennial Oscillation (QBO) is a teleconnection pattern that occurs in the tropical stratosphere. It is characterized by the almost periodic alternation between easterly and westerly winds, called, respectively, the easterly and westerly QBO phases (Ebdon, 1960, 1975; Reed et al., 1961). The cycle of zonal wind oscillation varies from 22 to 34 months, with an average of around 28 months (Baldwin et al., 2001). Naujokat (1986) described the main characteristics of QBO: the signal propagates downward to the lower stratosphere with time; the wind speed decreases at lower levels; the amplitude and the period of this oscillation change reasonably from cycle to cycle; the transition between easterly and westerly phases occurs between 30 and 50 hPa; the easterly QBO phase is, in general, more intense than the westerly one, and during the westerly phase, the winds propagate downwards faster, favoring the prevalence of this phase for a longer time in lower levels of the stratosphere. Although QBO is not literally a biennial oscillation, there is a preferential season for phase reversal. Considering the 50 hPa level, the onset of both the easterly and westerly phases occurs mainly in the late austral autumn (Dunkerton, 1990).

In the extratropics, the Annular Modes stand out as the leading mode of climate variability. This teleconnection pattern describes north-south "seesaws" of atmospheric mass between the high latitudes and parts of the midlatitudes in both hemispheres. In the Northern Hemisphere (NH), it is known as Arctic Oscillation (AO) or Northern Annular Mode (NAM), while it the Southern Hemisphere (SH), is named Antarctic Oscillation (AAO) or Southern Annular Mode (SAM). This pattern's structure is very similar for both hemispheres, occurring all months in the troposphere. The SAM reaches its "active phase" - maximum intensity in the stratosphere - at the end of austral spring, whereas for the NAM this stage occurs during the boreal winter. The positive (negative) Annular Mode phase is characterized by negative (positive) anomalies of geopotential height over polar regions and positive (negative) anomalies at mid-latitudes (Gong and Wang, 1999; Thompson and Wallace, 2000). This mode of variability is an active research area (Schenzinger and Osprey, 2015; Fogt and Marshall, 2020). The influence of lower frequency modes on SAM is a path to better knowledge about this pattern. Kodera and Koide (1997) and Baldwin and Dunkerton (1999) indicate that the typical NAM signal first appears in the stratosphere and then propagates downwards, suggesting that the NAM phase could be influenced by stratospheric circulation.

Although it is a tropical phenomenon, the QBO influence on the extratropical regions has been investigated by several authors, mainly in HN (e.g., Holton and Tan, 1980, 1982; Baldwin and Tung, 1994; Coughlin and Tung, 2001; Naoe and Shibata, 2010; Kuroda and Yamazaki, 2010; Roy and Haigh, 2011; Anstey and Shepherd, 2014; Li et al., 2020). Holton and Tan (1980) showed that the geopotential height at high latitudes is significantly lower during the westerly QBO phase. They suggested that the QBO may act either to focus planetary wave activity toward high latitudes or to allow its passage into the Tropics, through modulation of the latitudinal extent of the winter westerlies. The easterly QBO increases extratropical confinement of wave activity, weakening the vortex. The opposite situation during the westerly QBO, strengthens it (known as the Holton-Tan effect).

Studies relating QBO and Annular Modes have been carried out before, but they are generally focused on HN. Holton and Tan (1980), when examining 50 hPa geopotential composites in the NH, generated from the QBO phases, found a similar pattern to NAM. Coughlin and Tung (2001) showed a statistically significant relationship between the QBO signal and each level of the NAM, from 10 mb to 1000 mb, in which they all peak with the same frequency as the QBO. Other studies reveal that the positive (negative) NAM phase is associated with the westerly (easterly) QBO phase (e.g., Ruzmaikin et al., 2005; Scaife et al., 2014; Anstey and Shepherd, 2014). Kuroda and Yamazaki (2010) investigated the influence of the 11-year solar cycle and the QBO on the SAM in late winter/spring. They found that the SAM signal is strongly affected by both the solar cycle and the QBO. The SAM signal was restricted

to the troposphere and disappeared very quickly in years with low solar activity.

Several studies have indicated the separate influence of QBO (e.g., Gray, 1984; Mukherjee et al., 1985; Jury et al., 1994; Peings et al., 2013; Gray et al., 2018) and SAM (e.g., Gillett et al., 2006; Silvestri and Vera, 2003, 2009; Carvalho et al., 2005; Reboita et al., 2009; Vasconcellos and Cavalcanti, 2010; Blázquez and Solman, 2017; Rosso et al., 2018; Vasconcellos et al., 2019) around the globe. As discussed above, the QBO-NAM relationship has been addressed by previous studies, indicating an association between them. However, few studies show the association between QBO and SAM (e.g., Roy and Haigh, 2011; Anstey and Shepherd, 2014). It is, therefore, necessary to verify whether this relationship also occurs in the SH and investigate its variability, to better understand the variability of SAM.

In this study, we specifically focused on evaluating the possible relationship between QBO and SAM patterns through statistical analysis. As part of this investigation, the following questions were addressed:

1. Is there a relationship between QBO and SAM?
2. Does this relationship occur on all months?
3. Are there lags between them?

These questions were investigated by comparing QBO and SAM indices, the latter on different levels of the troposphere and stratosphere. The Continuous Wavelet Transform (CWT) and Cross Wavelet Transform (XWT) techniques were applied to identify significant common power and phase difference between the QBO and SAM. Contingency tables and composite analyses were also used to complement the study.

This paper is outlined as follows. Section 2 introduces the datasets and describes the methodology used to investigate the association between QBO and SAM. Section 3 presents and discusses the main findings. Summary and conclusions are presented in Section 4.

2. Dataset and Methods

Monthly datasets of ERA-Interim reanalysis from the European Centre for Medium Range Weather Forecasts (ECMWF) were used for the following variables: geopotential height at 700, 200, and 30 hPa, and zonal wind at 30 hPa. The daily ERA-Interim dataset was also used for air temperature and meridional wind at 30 hPa. ERA-Interim features a global spatial coverage, with a horizontal resolution of 0.5º x 0.5º latitude/longitude and 60 vertical levels from the surface to 0.1 hPa. Details on the data assimilation system of ERA-Interim can be found in Dee et al. (2011). The 1981-2010 period was evaluated. Monthly anomalies were constructed for each month by subtracting the corresponding 1981-2010 climatological monthly mean.

The QBO index was calculated based on Naujokat (1986): zonal mean (0º –360º) of 30 hPa zonal wind at 0º latitude. The index has negative values in the easterly QBO phase and positive values in the westerly QBO phase. The SAM indices were calculated for three different levels (troposphere and stratosphere): 700, 200, and 30 hPa. The index (for each level) was obtained from the principal component time series of geopotential height monthly anomaly polewards of 30ºS, using Empirical Orthogonal Function (EOF) (Vasconcellos et al., 2019). Positive (negative) values of the SAM index are associated with negative (positive) geopotential height anomalies over Antarctica and positive (negative) geopotential height anomalies at midlatitudes.

The wavelet transform can be used to analyze time series that contain nonstationary power at many different frequencies (Daubechies, 1990). Torrence and Compo (1998) indicate that the wavelet transform allows the identification of the dominant modes of variability with a more significant contribution to the signal observed in a given period. In time or space, the CWT has movable windows, which expand or compress to capture low and high-frequency signals, respectively. Thus, it becomes a useful tool to capture the contribution of each frequency to the time series, even if that contribution varies throughout the series (Labat, 2005). CWT was applied to the SAM index time series (for each level), to find the different scales that contribute to the SAM's large variability. The CWT figures display the time series on the X-axis and the frequency on the Y-axis. The cold colors represent less contribution to the series, and the warm colors are the frequencies that most contribute to the signal variability (high power). The CWT has edge

artifacts because the wavelet is not entirely localized in time. It is, therefore, useful to introduce a Cone of Influence (COI) in which edge effects cannot be ignored. Here, the region outside of COI is in blurred shade. The Monte Carlo test wats applied to find a 90% confidence level of the signal.

The XWT displays the regions in which the two time series vary together and reveals information about the relationship between their phases through phase vectors. It means that even if the relationship between the two signals does not occur simultaneously, the XWT can identify it. The XWT allows to identify the similarity between two signals, quantifying the degree of the relationship between them over time (Labat, 2005). The XWT was calculated using QBO and SAM indices (for each level). The figures obtained from the XWT are similar to those obtained with CWT. Peak power locations correspond to regions where the time series are related. The XWT figures also have arrows, the phase angles that indicate the lag between the two time series. To analyze the phase angles, it is necessary to know which time series was processed first, and in this case, QBO was the first. The phase relationship is shown as arrows, with in-phase pointing right, anti-phase pointing left, the QBO leading SAM by 90º (270º) pointing straight down (up). The toolbox based on the methodology described in Grinsted et al. (2004) was used to calculate both CWT and XWT (available in http://grinsted.github.io/wavelet-coherence/).

Further analysis was performed comparing QBO and SAM with no lag. The SAM is a result of the sum of influences at diverse time scale (Schenzinger and Osprey, 2015; Fogt and Marshall, 2020). As QBO is a low-frequency pattern, to compare these two series, the SAM index for each level was filtered to exclude high-frequency variability, using a moving average filter. The moving average is a simple linear filter that converts a series X_t, into another series Y_t, by the linear operation (Equation 1):

$$Y_t = \sum_{r=-q}^{s} a_r X_{t+r} \qquad (1)$$

where q and s represent the limits of the sum, and for this study q = s. X_t represents the series to be filtered, Y_t the resulting series, and a_r are the weights used in the moving average. In this study a_r is given by the expansion of the term $(1/2+1/2)^{2q}$. In this way,

the weight of the terms closest to the center is higher, giving them greater importance. For the 24-month (2-year) filter, the corresponding q is 12. However, for larger q values, the terms farther from the center get smaller and become negligible for the calculation. Therefore, when filtering the series, q = 4 was used, a sufficiently large value. This methodology was based on Chatfield (2004). Because of this q value, applying this filter to the first and last four months of the analyzed period is impossible. Thus, the filtered SAM index for the 1981 to 2010 period started in May 1981 and ended in August 2010.

Monthly contingency tables between the QBO and SAM (filtered) indices were created (without lag). The 2x2 tables were used. The upper-left square corresponds to the negative SAM phase events during the easterly QBO phase; the upper-right square corresponds to the negative SAM phase cases during the westerly QBO; the bottom-left square corresponds to the positive SAM phase along easterly QBO; and the bottom-right square corresponds to occurrences of a positive SAM phase along westerly QBO. These tables were created for each SAM index (700, 200, and 30 hPa). Because of the moving average filter, the contingency tables of January-April and September-December had 29 observations. The other months had 30 observations.

The correlation between the SAM index and zonal mean, both filtered using the moving average filter described above, was calculated to complement the results. The latitude versus pressure profile of this correlation was built. A t-student test (Wilks, 2006) was applied to composites at a 90% confidence level.

Geopotential height anomaly at 30 hPa and zonal wind were also filtered using the moving average filter described above. These were used to generate composite analyses for each QBO phase (without lag). The zonal wind was taken to create a latitude versus pressure profile (zonal mean). The geopotential height anomaly at 30 hPa was shown on a polar stereographic map. Also, we calculated the meridional heat flux ($v'T'$) at 30 hPa from the daily dataset and built composites for easterly and westerly QBO. Trenberth (1991) showed that the meridional heat flux ($v'T'$) is proportional to the Eliassen-Palm vertical component. Edmon et al. (1980) suggested the Eliassen-Palm flux components denote the direction and magnitude of the planetary wave propagation, so

30 hPa could be used as a measure of the activity of the waves entering the stratosphere. As for the other composites, the flux was also filtered.

Since November is the active period of SAM (Thompson and Wallace, 2000), we choose this month to analyze the correlation and composites described above. The periods used for these composites were identified with the CWT of the SAM index at 30 hPa (1987-1990 and 2000-2004, see Section 3 - Results). A t-student test (Wilks, 2006) was applied to composites and correlations at a 90% confidence level.

3. Results

As mentioned, the CWT technique was applied to SAM indices at 700, 200, and 30 hPa, and results are shown in Figure 1. Warm colors in Fig. 1 have higher power, corresponding to where most of the energy in the series is concentrated, and the black line represents the 95% significance level. The analysis of the 700 hPa SAM index (Fig. 1a) shows peak power in the 1-6 months band in several tyears of the time series, ceasing around 2007. It also presents high power regions in the 1-2 year band, for the periods: 1985-1990, 2000-2003 and 2007; a peak is also seen in the 4-6 year band, between 1993 and 2001. The CWT for the 500 hPa SAM index was quite similar to Figure 1a (not shown). In the upper troposphere (200hPa - Fig. 1b), the SAM index exhibited similar power peaks as in the lower troposphere, but generally for shorter periods. Peaks were observed in the 1-2 year band around 1989, 2000-2004 (this peak extended longer than 2-year band) and 2007. Significantly higher power in the 4-6 year band extended from approximately 1995 to 2001. The CWT obtained for the stratospheric SAM index (30 hPa) presented differences compared to tropospheric ones, as shown in Figure 1c. First, the significant peaks in power in the band up to 3 months were less frequent. Significant high power was observed in the bands around 6 months-1 year, 1-2 years (this peak also extended longer than 2 years), while the 4-6 years band had no significant power. Significant high power in the 1-2 year band was observed in periods 1987-1990 and 2000-2004. Fogt and Marshal (2019) discuss the variability in the SAM and show that this variability stems from changes in the extratropical

atmospheric circulation from the surface up through the stratosphere. Phenomena with several timescales can cause these changes, from synoptic (e.g., positive feedback between transient eddies and polar jet) to low-frequency modes (e.g., QBO and El Niño-Southern Oscillation), consistent with our CWT results.

Figure 1 revealed that the SAM index had several bands of high power, indicating many sources of variability. Schenzinger and Osprey (2015) and Fogt and Marshall (2020) also suggested sources with various timescales influencing the SAM. In addition, the SAM indices showed variability near the 2-year band for both the troposphere and stratosphere, suggesting that the QBO pattern could influence SAM variability in this band.

To verify this possibility, the XWT was applied between QBO and SAM indices (for 700, 200, and 30 hPa SAM indices). Figure 2a, corresponding to the XWT between QBO index and SAM index at 700 hPa, shows intense power peaks in the 2-year band around 1984-1985, 1988-1995, and from 1999 to the end of the time series. This result indicates an association between these two patterns in this band (approximately two years). When analyzing the phase vectors, lag phases can be seen between the QBO and SAM index time series. In the 2-year band (red rectangle) for the 1984-1985 period, the vectors are inclined approximately 90º (6 months lag) and 0º (in-phase), respectively. In the period 1988-1991, the phase vectors changed from 180º (anti-phase) to 90º (6 months lag). The 1992-1995 period had vectors in-phase (around 0º). In 1999, the patterns had 6 months lag (~90º) and, in 2000 became again in-phase (around 0º). The 2001-2004 period presented a higher phase difference, approximately 270º (18 months lag). From after 2004 until the end of the time series, the patterns were in phase (around 0º). The corresponding analysis with SAM index at 500 hPa (not shown) and 200 hPa (Fig. 2b) were similar to 700 hPa.

Some differences were observed in the stratospheric XWT (30 hPa - Fig. 2c) compared to the tropospheric ones (Fig. 2a-b). The high power observed in the stratosphere (around 2-year band) was more intense than in the troposphere. As in the troposphere, 1984 had about 6 months lag in the stratosphere. While in the stratosphere the period 1985-1987 was in phase, only 1985 was significant
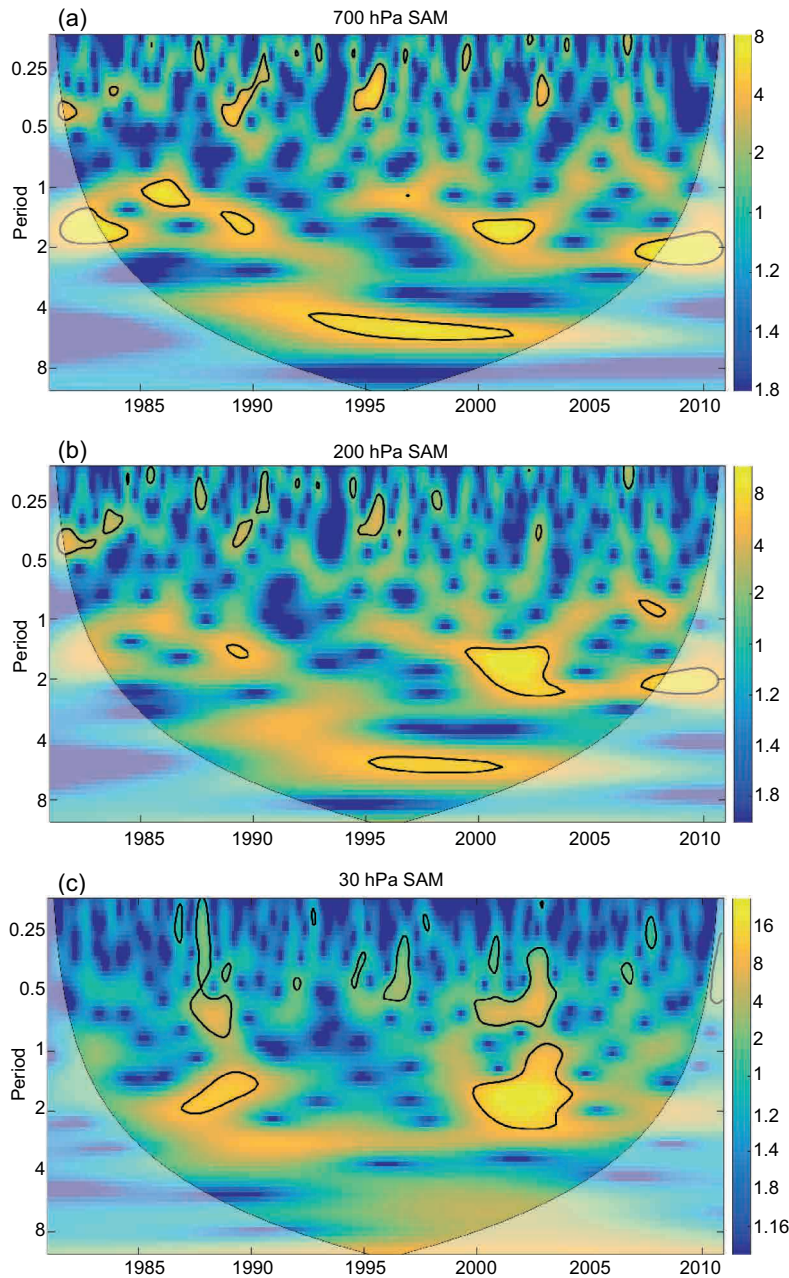
Fig. 1. Power spectrum of the continuous wavelet transform (CWT) of SAM index at: (a) 700 hPa, (b) 200 hPa, and (c) 30 hPa. The thick black contour designates the 5% significance level and the cone of influence (COI) where edge effects might distort the picture is shown as a blurred shade.

in the troposphere. In the 1988-1989 period, the vectors inclined approximately 270° (18 months lag) and 180° (anti-phase), respectively. Although the 2-year band had no significance in 1990-1992, there was a significant area right below 2-year (still within the QBO period) in which the arrows were in phase. The 1993-1996 and 1999 periods presented a 6-month lag (around 90°). In the 2000-2005 period, the vectors had a counterclockwise rotation, starting at 0° (in-phase), passing through the 270° (18-month
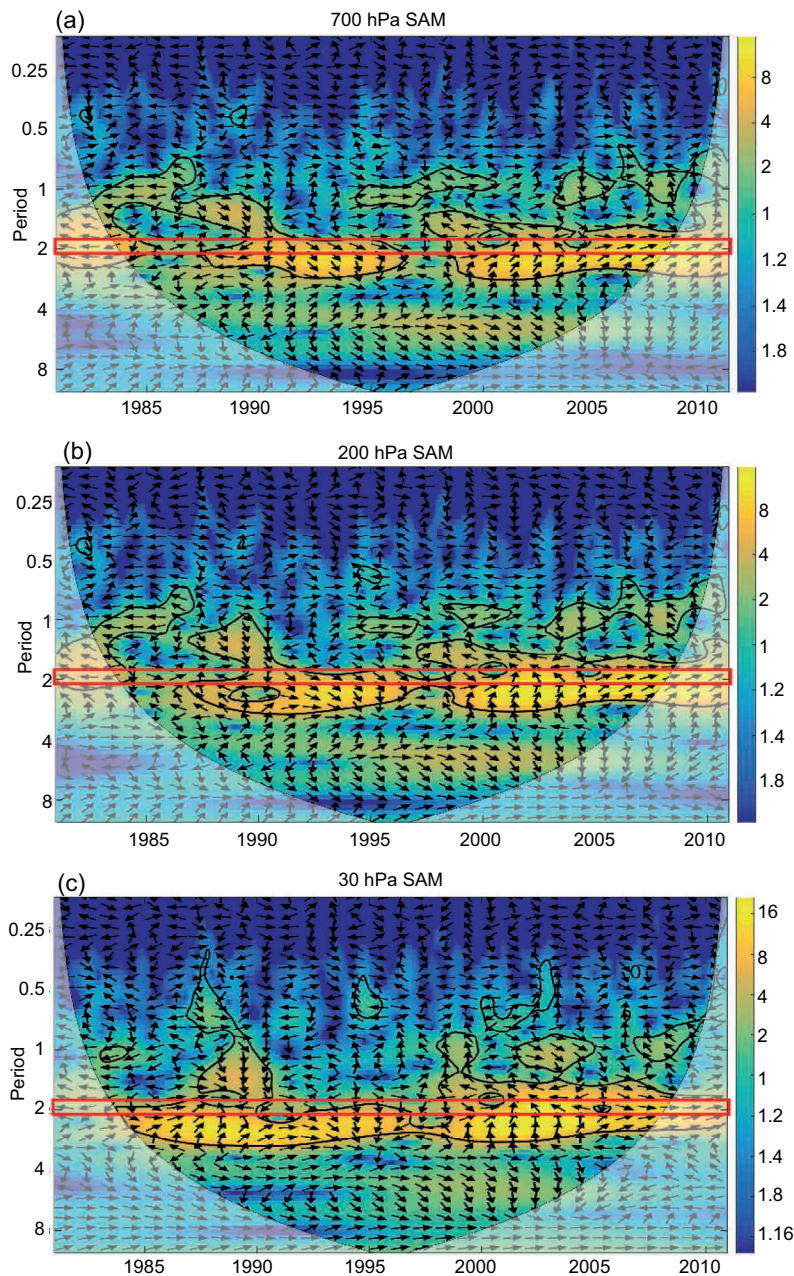
Fig. 2. Cross-wavelet transform (XWT) of the QBO and SAM index time series. The thick black contour designates the 5% significance level. The relative phase relationship is shown as arrows, with in-phase pointing right, anti-phase pointing left, the QBO leading SAM by 90º (270º) pointing straight down (up). The red rectangle displays the 2-year band.

lag) in 2001-20002, and 180º (anti-phase) in 2003-2004, finishing at 90º (6-month lag) in 2005. From 2006 onwards, the patterns were in phase (around 0º) as in the troposphere.

Figure 2 shows that there are different lags between QBO and SAM, including no lag; thus, we complement these results focusing on no lag. Monthly contingency tables counting the occurrences

of simultaneous cases (no lag) of QBO and SAM phases (filtered) are shown in Figures 3-5 (700, 200, and 30 hPa SAM index, respectively). It is noteworthy that the frequency of the SAM phases related to QBO phases varied slightly through the atmosphere. Perhaps this behavior occurred because the Annular Mode signal first appears in the stratosphere and propagates downwards with time (Kodera and Koide, 1997; Baldwin and Dunkerton, 1999), but that in the same month the propagation may not have yet reached the lowest levels. Additionally, Kuroda and Yamasaki (2010) indicate that the SAM signal stays restricted to the troposphere in years with low solar activity, which could also explain troposphere-stratosphere differences. It is necessary to observe the behavior of the SAM relative to the phases of QBO

JANUARY

SAM		QBO E	QBO W
	NEG	13	5
	POS	5	6

FEBRUARY

SAM		QBO E	QBO W
	NEG	8	8
	POS	7	6

MARCH

SAM		QBO E	QBO W
	NEG	6	8
	POS	6	9

APRIL

SAM		QBO E	QBO W
	NEG	5	8
	POS	8	8

MAY

SAM		QBO E	QBO W
	NEG	10	6
	POS	7	7

JUNE

SAM		QBO E	QBO W
	NEG	14	3
	POS	6	7

JULY

SAM		QBO E	QBO W
	NEG	12	4
	POS	9	5

AUGUST

SAM		QBO E	QBO W
	NEG	8	6
	POS	10	6

SEPTEMBER

SAM		QBO E	QBO W
	NEG	10	4
	POS	7	8

OCTOBER

SAM		QBO E	QBO W
	NEG	12	5
	POS	6	6

NOVEMBER

SAM		QBO E	QBO W
	NEG	10	5
	POS	8	6

DECEMBER

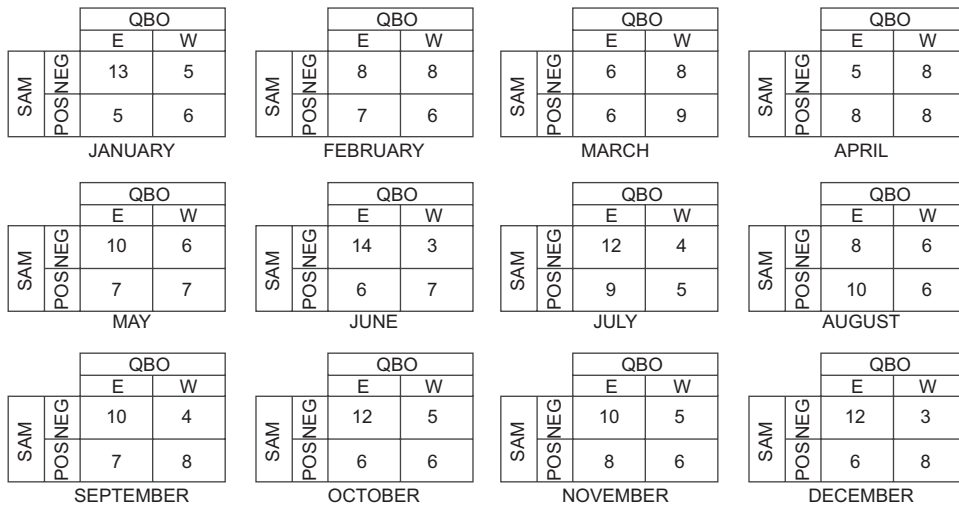| SAM		QBO E	QBO W
	NEG	12	3
	POS	6	8

Fig. 3. Monthly contingency tables between the QBO and SAM indices. SAM index (filtered) calculated for 700 hPa. The upper-left square corresponds to the events of the negative SAM phase during the easterly QBO phase (E); the upper-right square corresponds to the cases of negative SAM phase during the westerly QBO (W); the bottom-left square corresponds to events of positive SAM phase along easterly QBO (E); and the bottom-right square corresponds to occurrences of a positive SAM phase along westerly QBO (W).
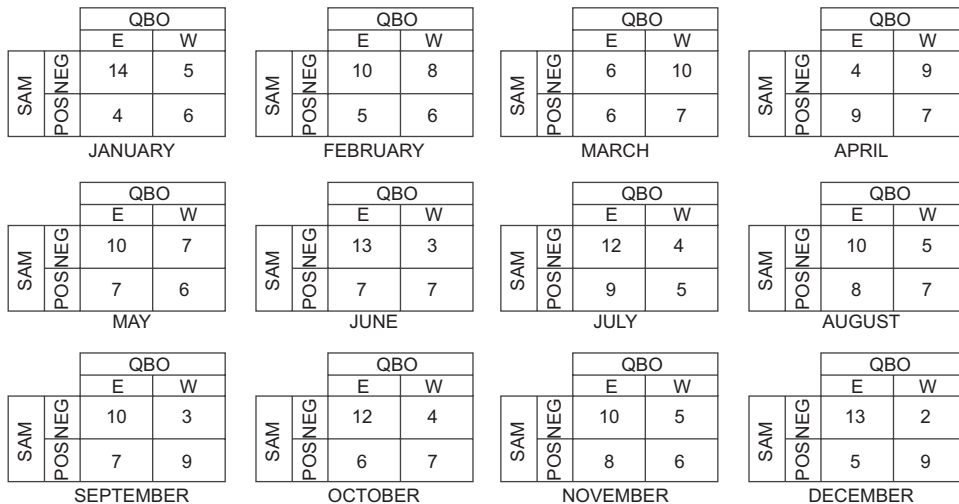
JANUARY

SAM		QBO E	QBO W
	NEG	14	5
	POS	4	6

FEBRUARY

SAM		QBO E	QBO W
	NEG	10	8
	POS	5	6

MARCH

SAM		QBO E	QBO W
	NEG	6	10
	POS	6	7

APRIL

SAM		QBO E	QBO W
	NEG	4	9
	POS	9	7

MAY

SAM		QBO E	QBO W
	NEG	10	7
	POS	7	6

JUNE

SAM		QBO E	QBO W
	NEG	13	3
	POS	7	7

JULY

SAM		QBO E	QBO W
	NEG	12	4
	POS	9	5

AUGUST

SAM		QBO E	QBO W
	NEG	10	5
	POS	8	7

SEPTEMBER

SAM		QBO E	QBO W
	NEG	10	3
	POS	7	9

OCTOBER

SAM		QBO E	QBO W
	NEG	12	4
	POS	6	7

NOVEMBER

SAM		QBO E	QBO W
	NEG	10	5
	POS	8	6

DECEMBER

SAM		QBO E	QBO W
	NEG	13	2
	POS	5	9

Fig. 4. Same as Figure 3, but for SAM index calculated at 200 hPa.

JANUARY

SAM \ QBO	E	W
POS	13	3
NEG	4	8

FEBRUARY

SAM \ QBO	E	W
POS	10	8
NEG	5	6

MARCH

SAM \ QBO	E	W
POS	3	12
NEG	9	5

APRIL

SAM \ QBO	E	W
POS	4	9
NEG	9	7

MAY

SAM \ QBO	E	W
POS	9	6
NEG	87	7

JUNE

SAM \ QBO	E	W
POS	11	5
NEG	9	5

JULY

SAM \ QBO	E	W
POS	11	4
NEG	10	5

AUGUST

SAM \ QBO	E	W
POS	12	3
NEG	6	9

SEPTEMBER

SAM \ QBO	E	W
POS	12	4
NEG	5	8

OCTOBER

SAM \ QBO	E	W
POS	12	4
NEG	6	7

NOVEMBER

SAM \ QBO	E	W
POS	12	4
NEG	6	7

DECEMBER

SAM \ QBO	E	W
POS	13	3
NEG	5	8

Fig. 5. Same as Figure 3, but for SAM index calculated at 30 hPa.

to analyze the contingency tables since the QBO is the longer-lasting phenomenon. Inspection of the columns in each table identified which SAM phase was more frequent in each QBO phase, to establish a relationship among them. When a SAM phase occurred more frequently during the easterly QBO and, during the westerly phase, the opposite SAM phase was more frequent ("oblique behavior" in the contingency tables), a relationship between the phenomena is suggested. Table I summarizes the results from the contingency tables (Figs. 3-5). The most frequent pattern presented the negative SAM phase related to the easterly QBO phase and the positive SAM phase associated with the westerly QBO phase. Months not included in the table did not present the "oblique behavior".

Table II – Classification of easterly and westerly QBO years (November) used for composite analysis (Figure 6). The period analyzed is 1987-1990 and 2000-2004.

Easterly QBO	Westerly QBO
1988, 1989, 2000, 2001, 2002, 2003	1987, 1990, 2004

November is the active SAM period (Thompson and Wallace, 2000), so we choose this month to analyze the latitude versus pressure profile of correlation between the SAM index and zonal wind (both filtered)

(Figure 6). The most significant correlations were found in the extratropics. This result was expected since the SAM is the leading mode of the extratropical region (Thompson and Wallace, 2000). The correlation map highlighted the relationship between SAM phase and the polar stratospheric vortex and polar night jet, showing a significant strengthening (weakening) of the stratospheric jet during positive (negative) SAM phase, as discussed in previous work (e.g., Thompson and Wallace, 2000; Fogt and Mar-
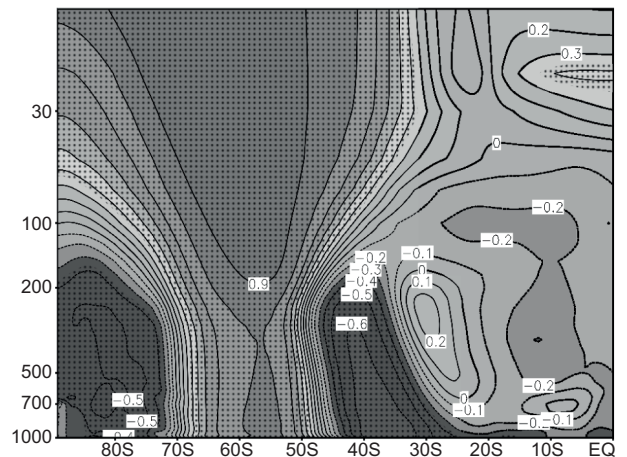

Fig. 6. Latitude versus pressure profile of correlation between the SAM index at 700 hPa and zonal wind (both filtered) for November. Areas with 90% significance are dotted (t-student test).
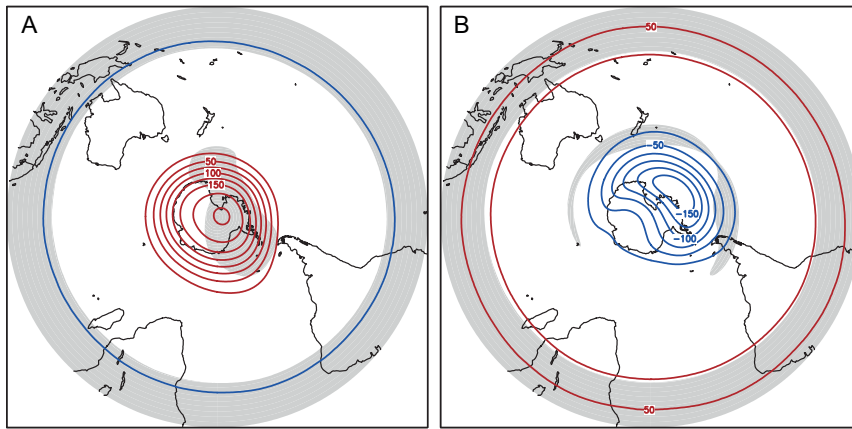
Fig. 7. Composite of geopotential height anomaly (m - filtered) for 30 hPa: (a) easterly QBO, and (b) westerly QBO. Contour interval of 25 m. Areas with 90% significance are shown in shaded (t-student test).

shall, 2019). There was also a significant positive correlation in the tropical stratosphere, i.e., positive (negative) SAM phase related to westerly (easterly) wind, although, at levels higher than 30hPa, this tropical region is dominated by the QBO. This result agreed with the contingency tables, indicating a relationship between positive (negative) SAM phase and westerly (easterly) QBO phase.

We also analyzed composites of geopotential height anomaly at 30 hPa for each QBO phase (Fig. 7). The period of these composites was identified from the CWT of the 30 hPa SAM index as no lag (1987-1990 and 2000-2004 - Fig. 2c). Table II shows the years used for each composite. Although there were few areas with statistical significance, the geopotential height anomaly composites displayed positive

(negative) anomalies at polar (middle) latitudes for easterly QBO phase, indicating negative SAM phase. The westerly QBO composite presented the opposite pattern, suggesting a positive SAM phase. These composites confirmed the results from the contingency tables.

Although the scope of this work was not to investigate the mechanisms of the QBO-SAM relationship, a possible cause of this link is wave propagation to the stratosphere, which affects the QBO and the polar stratospheric vortex (e.g., Baldwin and Tung, 1994; Thompson and Wallace, 2000; Fogt and Marshall, 2019; Li et al., 2020). The maximum of this wave propagation from the troposphere to the stratosphere in the SH occurs in late spring (Charney and Drazin, 1961; Randel and Newman, 1998). To corroborate

Table I – Summary of results presented in the monthly contingency tables (Fig. 3-5). Months not included in the table are those that do not present the "oblique behavior".

	Easterly QBO/negative SAM Westerly QBO/positive SAM	Easterly QBO/positive SAM Westerly QBO/negative SAM
700 hPa SAM index	January, May, June, July, September, October, November, December	-
200 hPa SAM index	January, June, July, August, September, October, November, December	April
30 hPa SAM index	January, May, July, August, September, October, November, December	March, April

this hypothesis, we analyzed the composites of meridional heat flux at 30 hPa for November (Fig. 8). The composites were built for the period described in Table II. Edmon et al. (1980) discussed the role Eliassen-Palm flux components to identify the direction and magnitude of the planetary wave propagation. The meridional heat flux is proportional to the Eliassen-Palm vertical component (Trenberth, 1991), and it can be used to measure the activity of the waves entering the stratosphere. Maximum negative values occurred at 60ºS, and there was almost no difference between QBO phases at this latitude (Fig. 8). However, at higher latitudes where the polar stratospheric vortex was located, the easterly QBO displayed stronger values, which suggested there was more wave propagation to the stratosphere in this phase, compared to westerly QBO. Li et al. (2020) also indicated stronger (weaker) upward wave propagation to the stratosphere with easterly (westerly) QBO and linked this to the polar stratospheric vortex. The wave develops in the troposphere and propagates vertically into the stratosphere along the jet core axis. The wave decelerates the stratospheric polar jet by depositing easterly momentum into the westerly stratospheric jet (Charney and Drazin, 1961; Edmon et al., 1980; Randel and Newman, 1998; Kuroda and Yamazaki, 2010). Figure 9 confirmed the
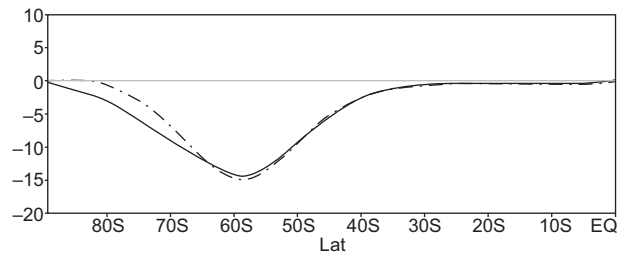
Fig. 8. Composite of zonal mean meridional heat flux (K ms^{-1}) for 30 hPa. Solid line: easterly QBO, and dot dashed line: westerly QBO.

stratospheric jet weakening in the easterly QBO composite. A weak (strong) stratospheric jet is associated with a negative (positive) SAM phase (Thomson and Wallace, 2000; Fogt and Marshall 2020). The results presented above confirmed the relationship between QBO and SAM and indicated upward wave propagation to the stratosphere at high latitudes as a possible mechanism.

4. Summary and conclusions

The SAM pattern influences climate over the SH (e.g., Gillett et al., 2006; Silvestri and Vera, 2003, 2009; Vasconcellos et al., 2019). However, the varia-
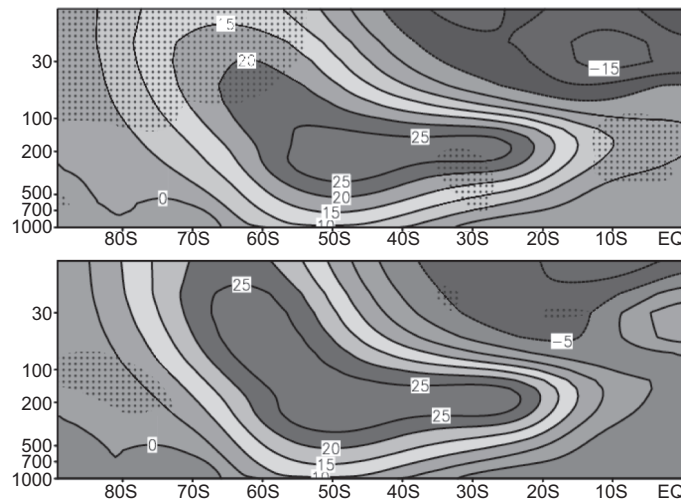

Fig. 9. Latitude versus pressure profile of composite of zonal mean zonal wind (ms^{-1} - filtered): (top) easterly QBO, and (bottom) westerly QBO. Areas with 90% significance are dotted (t-student test).

bility of this mode is an active area of research. The influence of lower frequency modes on SAM is a path to better knowledge about its variability. While prior works have studied the relationship between QBO and NAM, few studies showed an association between QBO and SAM. This study confirmed that this relationship also occurs in the SH and investigated the variability associated with this relation.

CWT applied to SAM indices in the troposphere and stratosphere, showed power peaks for different bands, including around 2 years. In the stratosphere (30 hPa), the significantly higher power around the 2-year band was seen for the periods 1987-1990 and 2000-2004. This result indicated SAM index had variability at various scales, including two-years, possibly because of the QBO influence. The XWTs analysis between the QBO and SAM indices revealed significant common high power around the 2-year band for all the results obtained. However, this band showed lag variations between the QBO and SAM series over the analyzed period, including no lag., suggesting that the influence of the QBO on the SAM could happen simultaneously and several months later.

Focusing on the QBO influence on the SAM with no lag, we built monthly contingency tables between the QBO index and the SAM indices at different levels (30, 200, and 700 hPa - filtered, without lags). These results showed that, for most of the months, during the QBO easterly phase, there was a higher occurrence of the negative SAM phase. Alternatively, during the QBO westerly phase, there was a higher occurrence of the positive SAM phase. This relationship between QBO and SAM is consistent with previous results (e.g., Roy and Haigh, 2011; Anstey and Shepherd, 2014). Nevertheless, this study showed that this relationship is not valid for all months. Composite analyses for each QBO phase (period described at 30 hPa SAM`s CWT) were performed for the SAM active period (November), confirming the results from the contingency tables. More (less) upward wave propagation into the stratosphere at high latitudes for easterly (westerly) QBO phase, weakening (strengthens) the stratospheric polar vortex, leading to negative SAM phase. These results agree with results by Fogt and Marshall (2020) and Li et al. (2020).

This study confirmed that there is a relationship between the QBO and the SAM. It also showed various lags between these two patterns, suggesting that this relation has a complex interaction. Nevertheless, analyses without lag indicated that the negative (positive) SAM phase was more frequent for easterly (westerly) QBO in most (but not all) months, including the SAM active period (November). It lies beyond the scope of this study to determine the physical mechanisms associated with the influence of QBO on SAM. However, some additional analysis indicated that the upward wave propagation to the stratosphere for each QBO phase modifies the stratospheric jet and, consequently, the SAM phase. This study provides insight on SAM variability and its predictability. Further research is ongoing and will be presented in future publications.

References

Anstey JA, Shepherd TG. 2014. High-latitude influence of the quasi-biennial oscillation. Quarterly Journal of the Royal Meteorological Society 140: 1-21. https://doi.org/10.1002/qj.2132

Baldwin MP, Dunkerton TJ. 1999. Propagation of the Arctic Oscillation from the stratosphere to the troposphere. Journal of Geophysical Research 104: 30937-30946. https://doi.org/10.1029/1999JD900445

Baldwin MP, Gray LJ, Dunkerton TJ, Hamilton K, Haynes PH, Randel WJ, Holton JR, Alexander MJ, Hirota I, Horinouchi T, Jones DBA, Kinnersley JS, Marquardt C, Sato K, Takahashi M. 2001. The quasi-biennial oscillation. Reviews of Geophysics 39: 179- 229. https://doi.org/10.1029/1999RG000073

Baldwin MP, Tung KK. 1994. Extra-tropical QBO signals in angular momentum and wave forcing. Geophysical research letters 21: 2717-2720. https://doi.org/10.1029/94GL02119

Blázquez J, Solman SA. 2017. Interannual variability of the frontal activity in the Southern Hemisphere: rela-

tionship with atmospheric circulation and precipitation over southern South America. Climate Dynamics 48: 2569-2579. https://doi.org/10.1007/s00382-016-3223-3

Carvalho LMV, Jones C, Ambrizzi T. 2005. Opposite phases of the Antarctic Oscillation and relationships with intraseasonal to interannual activity in the tropics during the austral summer. Journal of Climate 18: 702-718. https://doi.org/10.1175/JCLI-3284.1

Charney JG, Drazin PG. 1961. Propagation of planetary-scale disturbances from the lower into the upper atmosphere. Journal of Geophysical Research 66: 83-109. https://doi.org/10.1029/JZ066i001p00083

Chatfield C. 2004. The Analysis of Time Series: An introduction. Boca Raton, FL: Chapman and Hall/CRC.

Coughlin K, Tung, KK. 2001. QBO signal found at the extratropical surface through northern annular modes. Geophysical Research Letters 28: 4563-4566. https://doi.org/10.1029/2001GL013565

Dee DP, Uppala SM, Simmons AJ, Berrisford P, Poli P, Kobayashi S, Andrae U, Balmaseda MA, Balsamo G, Bauer P, Bechtold P, Beljaars ACM, van de Berg L, Bidlot J, Bormann N, Delsol C, Dragani R, Fuentes M, Geer AJ, Haimberger L, Healy SB, Hersbach H, Hólm EV, Isaksen L, Kållberg P, Köhler M, Matricardi M, McNally AP, Monge-Sanz BM, Morcrette JJ, Park BK, Peubey C, de Rosnay P, Tavolato C, Thépaut JN, Vitart F. 2011. The ERA-Interim reanalysis: configuration and performance of the data assimilation system. Quarterly Journal of the Royal Meteorological Society 137: 553-597. https://doi.org/10.1002/qj.828

Daubechies I. 1990. The wavelet transform time-frequency localization and signal analysis. IEEE Transactions on Information Theory 36: 961-1004. https://doi.org/10.1109/18.57199

Dunkerton TJ. 1990. Annual variation of deseasonalized mean flow acceleration in the equatorial lower stratosphere. Journal of the Meteorological Society of Japan 68: 499-508. https://doi.org/10.2151/jmsj1965.68.4_499

Ebdon RA. 1975. The quasi-biennial oscillation and its association with tropospheric circulation patterns. Meteorological Magazine 104: 282-297.

Edmon HJ, Hoskins BJ, Mcintyre ME. 1980. Eliassen-palm cross section for the troposphere. Journal of Atmospheric Sciences 37: 2600-2616. https://doi.org/10.1175/1520-0469(1980)037<2600:EPCSFT>2.0.CO;2

Fogt RL, Marshall, GJ. 2020. The Southern Annular Mode: Variability, trends, and climate impacts across the Southern Hemisphere. WIREs Climate Change 11: e652. https://doi.org/10.1002/wcc.652

Gillett NP, Kell TD, Jones PD. 2006. Regional climate impacts of the Southern Annular Mode. Geophysical Research Letters 33: L23704. https://doi.org/10.1029/2006GL027721

Gong D, Wang S. 1999. Definition of Antarctic Oscillation index. Geophysical Research Letters 26: 459–462. https://doi.org/10.1029/1999GL900003

Gray WM. 1984. Atlantic seasonal hurricane frequency. Part I: El Niño and 30 mb Quasi Biennial Oscillation influences. Monthly Weather Review 112: 1649-1668. https://doi.org/10.1175/1520-0493(1984)112<1649:ASHFPI>2.0.CO;2

Gray LJ, Anstey JA, Kawatani Y, Lu H, Osprey S, Schenzinger V. 2018. Surface impacts of the Quasi Biennial Oscillation. Atmospheric Chemistry and Physics 18: 8227-8247. https://doi.org/10.5194/acp-18-8227-2018

Grinsted A, Moore JC, Jevrejeva S. 2004. Application of the cross wavelet transform and wavelet coherence to geophysical time series. Nonlinear Processes in Geophysics 11: 561-566. https://doi.org/10.5194/npg-11-561-2004

Holton JR, Tan H. 1980. The influence of the equatorial Quasi-Biennial Oscillation on the global circulation at 50 mb. Journal of the Atmospheric Sciences 37: 2200-2208. https://doi.org/10.1175/1520-0469(1980)037<2200:TIOTEQ>2.0.CO;2

Holton JR, Tan H. 1982. The Quasi-Biennial Oscillation in the Northern Hemisphere lower stratosphere. Journal of the Meteorological Society of Japan 60: 140-148. https://doi.org/10.2151/jmsj1965.60.1_140

Jury MR, Mc Queen C, Levey K. 1994. SOI and QBO signals in the African region. Theoretical and Applied Climatology 50: 103-115. https://doi.org/10.1007/BF00864907

Kodera K, Koide H. 1997. Spatial and seasonal characteristics of recent decadal trends in the northern hemispheric troposphere and stratosphere. Journal of Geophysical Research 102: 19443-19447. https://doi.org/10.1029/97JD01270

Kuroda Y, Yamazaki K. 2010. Influence of the solar cycle and QBO modulation on the Southern Annular Mode. Geophysical Research Letters 37: L12703. https://doi.org/10.1029/2010GL043252

Labat, D. 2005. Recent advances in wavelet analyses: Part 1. A review of concepts. Journal of Hydrology

314: 275 – 288, 2005. https://doi.org/10.1016/j.jhydrol.2005.04.003

Li Z., Chu X, Harvey VL, Jandreau J, Lu X, Yu Z, Zhao J, Fong W. 2020. First lidar observations of Quasi-Biennial Oscillation-induced interannual variations of gravity wave potential energy density at McMurdo via a modulation of the Antarctic polar vortex. Journal of Geophysical Research 125: 22p. https://doi.org/10.1029/2020JD032866

Mukherjee BK, Indira K, Reddy RS, Murty BVR. 1985. Quasi-Biennial Oscillation in Stratospheric Zonal Wind and Indian Summer Monsoon. Monthly weather review 113: 1421-1424. https://doi.org/10.1175/1520-0493(1985)113<1421:QBOISZ>2.0.CO;2

Naoe H, Shibata K. 2010. Equatorial quasi-biennial oscillation influence on northern winter extratropical circulation. Journal of Geophysical Research 115: D19102. https://doi.org/10.1029/2009JD012952

Naujokat B. 1986. An update of the observed quasi-biennial oscillation of the stratospheric winds over the tropics. Journal of the Atmospheric Sciences 43: 1873-1877. https://doi.org/10.1175/1520-0469(1986)043<1873:AUOTOQ>2.0.CO;2

Peings Y, Brun E, Mauvais V, Douville H. 2013. How stationary is the relationship between Siberian snow and Arctic Oscillation over the 20th century? Geophysical Research Letters 40: 183-188. https://doi.org/10.1029/2012GL054083

Reboita MS, Ambrizzi T, Rocha RP. 2009. Relationship between the southern annular mode and southern hemisphere atmospheric systems. Revista Brasileira de Meteorologia 24: 48-55. https://dx.doi.org/10.1590/S0102-77862009000100005

Reed RJ, Campbell WJ, Rasmussen LA, Rogers DG. 1961. Evidence of a downward-propagating, annual wind reversal in the equatorial stratosphere. Journal of Geophysical Research 66: 813-818. https://doi.org/10.1029/JZ066i003p00813

Randel WJ, Newman PA. 1998. The stratosphere in the southern hemisphere. In: Karoly DJ, Vincent DG (eds) Meteorology of the Southern Hemisphere. Meteorological Monographs, American Meteorological Society, Boston, MA. https://doi.org/10.1007/978-1-935704-10-2_9

Rosso FV, Boiaski NT, Ferraz SET, Robles TC. 2018. Influence of the Antarctic Oscillation on the South Atlantic Convergence Zone. Atmosphere 9: 431. https://doi.org/10.3390/atmos9110431

Roy I, Haigh JD. 2011. The influence of solar variability and the quasi-biennial oscillation on sea level pressure. Atmospheric Chemistry and Physics 11: 11679-11687. https://doi.org/10.5194/acp-11-11679-2011

Ruzmaikin A, Feynman J, Jiang X, Yung YL. 2005. Extratropical signature of the quasi-biennial oscillation. Journal of Geophysical Research 110: D11111. https://doi.org/10.1029/2004JD005382

Scaife AA, Athanassiadou M, Andrews M, Arribas A, Baldwin M, Dunstone N, Knight J, MacLachlan C, Manzini E, Müller WA, Pohlmann H, Smith D, Stockdale T, Williams A. 2014. Predictability of the quasi-biennial oscillation and its northern winter teleconnection on seasonal to decadal timescales. Geophysical Research Letters 41: 1752 - 1758. https://doi.org/10.1002/2013GL059160

Schenzinger V, Osprey SM. 2015. Interpreting the nature of Northern and Southern Annular Mode variability in CMIP5 Models. Journal of Geophysical Research 120: 11,203-11,214. https://doi.org/10.1002/2014JD022989

Silvestri GE, Vera CS. 2003. Antarctic oscillation signal on precipitation anomalies over southeastern South America. Geophysical Research Letters 30: 2115-2118. https://doi.org/10.1029/2003GL018277

Silvestri GE, Vera CS. 2009. Nonstationary impacts of the southern annular mode on southern hemisphere climate. Journal of Climate 22: 6142-6148. https://doi.org/10.1175/2009JCLI3036.1

Thompson DW, Wallace JM. 2000. Annular modes in the extratropical circulation. Part I: Month-to-month variability. Journal of climate 13: 1000-1016. https://doi.org/10.1175/1520-0442(2000)013<1000:AMITEC>2.0.CO;2

Trenberth KE. 1991. Storm Track in the Southern Hemisphere. Journal of the Atmospheric Sciences 48: 2159-2178. https://doi.org/10.1175/1520-0469(1991)048<2159:STITSH>2.0.CO;2

Torrence C, Compo GP. 1998. A practical guide to wavelet analysis. Bulletin of American Meteorological Society 79: 61-78. https://doi.org/10.1175/1520-0477(1998)079<0061:APGTWA>2.0.CO;2

Vasconcellos FC, Cavalcanti IFA. 2010. Extreme precipitation over Southeastern Brazil in the austral summer and relations with the Southern Hemisphere annular mode. Atmospheric Science Letters 11: 21-26. https://doi.org/10.1002/asl.247

Vasconcellos FC, Pizzochero RM, Cavalcanti IFA. 2019. Month-to-month impacts of Southern Annular Mode

over South America climate. Anuário de Instituto de Geociências da UFRJ 42: 783-792. http://dx.doi.org/10.11137/2019_1_783_792

Wilks DS. 2006. Statistical Methods in the Atmospheric Sciences. San Diego, CA: Academic Press (International Geophysics Series, v. 91).